



## Research Article

# Design of a Lens System Reduces Chromatic Aberration for Proton Radiography

Qinggang Jia <sup>1</sup>, Wenyuan Wang,<sup>1</sup> Haibo Xu,<sup>1</sup> and Liang Lu <sup>2,3</sup>

<sup>1</sup>*Institute of Applied Physics and Computational Mathematics, No. 6, Hua-Yuan Road, Hai-Dian District, Beijing, China*

<sup>2</sup>*Sino-French Institute of Nuclear Engineering and Technology, Sun Yat-Sen University, Zhuhai 519082, Guangdong, China*

<sup>3</sup>*Institute of Modern Physics, Chinese Academy of Sciences, Lanzhou 730000, China*

Correspondence should be addressed to Qinggang Jia; [qgjia\\_xjtu@126.com](mailto:qgjia_xjtu@126.com)

Received 2 December 2021; Revised 26 April 2022; Accepted 10 May 2022; Published 11 June 2022

Academic Editor: Dimitri Batani

Copyright © 2022 Qinggang Jia et al. This is an open access article distributed under the Creative Commons Attribution License, which permits unrestricted use, distribution, and reproduction in any medium, provided the original work is properly cited.

Multi-GeV proton radiography is an important tool for diagnosing density distribution of thick objects. The magnetic lens system called Zumbro lens is widely employed because it compensates for the image distortion induced by small angle multiple Coulomb scattering (MCS) that occurs when the charged protons passing through the object. However, radiography is still suffering from chromatic aberration induced blurring, if the momentum of transmitted proton is different from the reference value of Zumbro lens. In this paper, two methods are employed to reduce chromatic aberration. The first is based on magnetic lens optimization. In addition, a new lens system is first proposed locating the downstream of Zumbro. It is named “auxiliary” lens, which can correct the chromatic aberration for certain protons with momentum far away from the reference of Zumbro lens. Monte Carlo simulation shows that this proposed lens can decrease chromatic aberration and improve the radiography image evidently.

## 1. Introduction

Compared to X-ray, the multi-GeV high-energy proton owning extreme penetrating power performs better as a radiographic probe for dense objects [1–8]. However, proton experiences multiple Coulomb scattering (MCS) when it passes through the material. This MCS effect will seriously blur the radiographic image of the object. To suppress this kind of blurring, a magnetic structure called Zumbro lens was developed by Mottershead and Zumbro [1], which is now the most important part of the proton radiography system.

Zumbro lens is designed according to the momentum of the transmitted proton [8, 9]. Then, the lens can provide a point-to-point focus from the object to image without blurring for protons whose momentum is the same as the reference value. However, once the object has a wide range of areal densities, the momentum of transmitted protons spreads to a large range. This momentum spreading leads to chromatic aberration when the proton transfers in the magnetic lens. Then, unexpected blurring and distortion induced by

chromatic aberration can be found on the image. Moreover, because the areal density of the object is unknown in experiments, the designed reference momentum may widely differ from that of the transmitted proton. In this situation, extra undesired chromatic aberration will be introduced.

Blurring induced by chromatic aberrations significantly degenerates the imaging resolution [10]. It varies spatially determined by object areal densities and consequent proton energy loss. Admittedly, this kind of blurring can highlight the location of boundary [11]. Especially for dark field radiography, the discontinuity of object is evidently enhanced, as shown in Figure 5 of Ref [12]. However, additional image distortion brought by chromatic aberrations can adversely affect quantitative analysis of the object.

According to Ref. [1], reduction about chromatic aberrations can be achieved by three methods. The first is by improving the proton momentum. 70 GeV proton facilities are reported [13]. Second, shielding the protons with a large scattered angle can theoretically suppress chromatic aberrations. However, no related study is reported for this

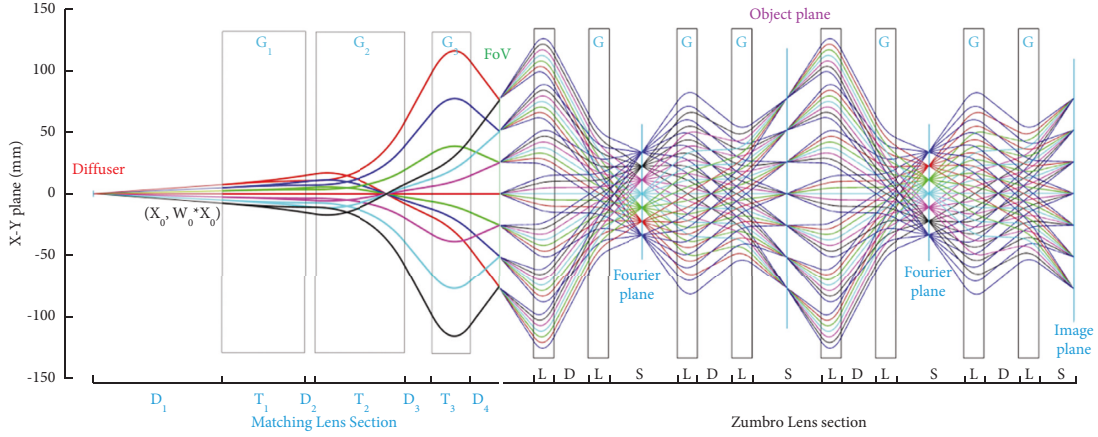


FIGURE 1: Layout of proton beam in radiography system.

purpose. Ref. [8] discusses collimation and angle cut for the purpose of density reconstruction.

The last but very important is Zumbro lens optimization for chromatic aberrations reduction. Thin-lens approximation is applied [14] for lens optimization. Some software such as WinAGILE [15] and COSY INFINITY [16, 17] can be used to search the lens parameter. However, not only Zumbro lens but also the matching lens and diffuser should be optimized as a whole system. This is a very complicated optimization because many constraints should be considered during parameter searching. There is no such report about imaging system optimization. In addition, there is only one reference momentum of Zumbro lens. For protons far away from the reference momentum, particularly for thick objects, chromatic aberration cannot be removed even with an optimized system.

In this paper, we describe the optimal design of the Zumbro lens, the matching lens, and the diffuser. The optimization has a large, multidimensional searching space. Moreover, several constraints such as field of view (FOV) and inverting-identity imaging directly affect the searching of the best solution. The genetic algorithm [18, 19] (GA) is therefore employed empirically to solve this optimization problem. Besides system optimization, a lens named “auxiliary” is first proposed to further decrease chromatic aberrations. This lens locates downstream the Zumbro lens. It is optimized to refocus the proton whose momentum is away from the reference value. A slab and a sphere which contain vacancies inside are taken as the test objects to verify the performance by Monte Carlo Geant4 [20] simulation. The results show that the chromatic aberrations can be evidently decreased by using the Zumbro lens and the proposed auxiliary lens.

## 2. Radiography System Optimization

**2.1. Proton Radiography System.** The basic configuration of the proton radiography system consists of three key parts: the diffuser, matching lens, and Zumbro lens. The proton beam whose direction is from left to right in system is shown in Figure 1. A pencil mono-energy proton beam is firstly scattered in a diffuser. With a broader angular distribution, it

transfers in to matching lens. Both the angle and size of the beam are modified in matching lens according to the coordinate-angle correlation required by Zumbro lens. Then, the protons with this correlation can be imaged by Zumbro lens when it reaches the image plane as shown in Figure 1.

**2.2. Zumbro Magneto-Optical Lens.** The MCS and proton-nucleus elastic scattering result in a random direction of the protons as they leave the object. This effect blurs the recorded image. In addition to this, due to the stopping of object material, the proton energy spreads when it exits the object. This energy spreading leads to chromatic aberration when the proton transfers in the magnetic lens. The chromatic aberration finally blurs the recorded image. The Zumbro lens can remove the blur caused by MCS, as well as the first order of chromatic aberration. According to Ref. [1], the rest second-order chromatic aberrations term  $Err_c$  has the following form:

$$Err_c = m'_{12} \cdot \phi \cdot \sigma, \quad (1)$$

where  $\phi$  is the angular deviation from the ideal position-angle correlation line and  $\sigma$  is the fractional momentum deviation. Both  $\phi$  and  $\sigma$  scale inversely with the beam momentum. Therefore, the higher the proton energy, the lower the chromatic aberrations will be. Once the proton beam and object are set,  $Err_c$  is proportional to the value of  $m'_{12}$ , regardless of collimation and angle cut. In this case, better resolution is therefore expected with lower  $m'_{12}$ . The optimization of Zumbro lens is to minimize the value of  $m'_{12}$ .

**2.2.1. Goal of Optimization.** As shown in Figure 1, Zumbro lens has two same subsections. Each one consists of eight quadrupoles. In the simplest case, the transfer matrix  $MZ$  of one section can be described [21] by four parameters, quadrupole length ( $L/m$ ) and strength ( $G/\text{tesla} \cdot m^{-1}$ ), the inside drifts ( $D/m$ ), and the outside drifts ( $S/m$ ):

$$MZ = \begin{vmatrix} m_{11}(L, G, S, D) & m_{12}(L, G, S, D) \\ m_{21}(L, G, S, D) & m_{22}(L, G, S, D) \end{vmatrix}. \quad (2)$$

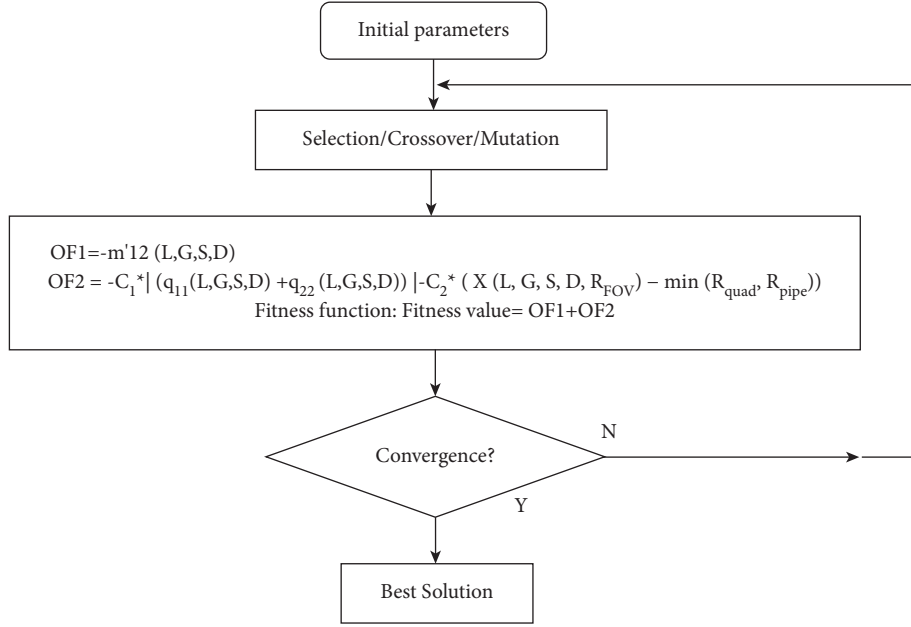


FIGURE 2: The flowchart of optimization with GA.

Because the expression of  $m'_{12}$  is an implicit function, an approximate calculation is used that  $m'_{12} = (m_{12}(L, G, S, D, E) - m_{12}(L, G, S, D, E - \Delta E)) / \Delta E$ . The goal of optimization is to minimize  $m'_{12}$ .

**2.2.2. Optimization Constraints.** During the searching of the best parameter set, several constraints should be taken into consideration. The first one is unit-magnification point-to-point inverting identity lens constraint for both  $x$  or  $y$  coordinate plane (beam along  $z$  axis). So, this constraint imposed on the optimization can be expressed by the following:

$$MZ = \begin{vmatrix} m_{11}(L, G, S, D) & m_{12}(L, G, S, D) \\ m_{21}(L, G, S, D) & m_{22}(L, G, S, D) \end{vmatrix} = \begin{vmatrix} -1 & 0 \\ 0 & -1 \end{vmatrix}, \quad (3)$$

Indeed, the transfer matrix  $MZ$  is formed by a pair of the same symmetric submatrix [14] that  $MZ = MZ_{\text{sub}} * MZ_{\text{sub}}$ . Each submatrix describes the transmission of proton in one half of Zumbro lens. The submatrix is written in the following form:

$$MZ_{\text{sub}} = \begin{vmatrix} q_{11}(L, G, S, D) & q_{12}(L, G, S, D) \\ q_{21}(L, G, S, D) & q_{22}(L, G, S, D) \end{vmatrix}. \quad (4)$$

The constraints of inverting identity can be given as follows:

$$q_{11}(L, G, S, D) + q_{22}(L, G, S, D) = 0. \quad (5)$$

The FOV is another important constraint. As shown in Figure 1, the proton in FOV should not hit the aperture of magnetic iron or beam pipe when it travels all the way through the lens system. To make it clear for optimization, the Zumbro lens is divided into two fictitious segments arbitrarily. The transfer of an initial proton in the upstream segment can be expressed in the following form:

$$\begin{pmatrix} X \\ X' \end{pmatrix} = \begin{vmatrix} Um_{11} & Um_{12} \\ Um_{21} & Um_{22} \end{vmatrix}_{\text{Upstream}} \begin{pmatrix} X_0 \\ w * X_0 + \phi \end{pmatrix}_{\text{FOV}}, \quad (6)$$

where  $\begin{vmatrix} Um_{11} & Um_{12} \\ Um_{21} & Um_{22} \end{vmatrix}_{\text{Upstream}}$  is the transfer matrix of upstream segment. At the end of the upstream segment,  $X$  and  $X'$  are the coordinate and trajectory angle of the proton, respectively. The coordinate  $X$  at any arbitrary divisional plane can be calculated by lens parameters and initial coordinate  $X_0$ . The calculated value of  $X$  should be smaller than the inner radius of the quadrupole or beam pipe. As shown in Figure 1, protons located at the edge of FOV have a trace whose coordinate  $X$  may reach the maximum. Therefore, the constraint that protons are transmitted without bombarding magnetic iron or beam pipe can be expressed as formula (7). Here, the minimum value of  $R_{\text{quadrupole}}$  and  $P_{\text{pipe}}$  is set to be 12 cm.

$$\begin{aligned} |X(L, G, S, D, X_0)| &< \min(R_{\text{quadrupole}}, R_{\text{pipe}}) \\ &= 12\text{cm} (X_0 = R_{\text{FOV}}). \end{aligned} \quad (7)$$

**2.2.3. Optimization Method: Genetic Algorithm.** In the aspect of optimization, two constraints for four parameters mean a large space of allowed solutions. The traditional design method of magnetic is based on thin-lens approximation. It takes the size of FOV as a posterior limitation on the parameters. However, this approximation may not provide the best solution.

All the constraints should be taken as object functions to guarantee a reasonable result. The design is expected to be a multiobjective optimization. The genetic algorithm (GA) is recognized as the best globally well-adapted optimization algorithm. It has been successfully employed to deal with the

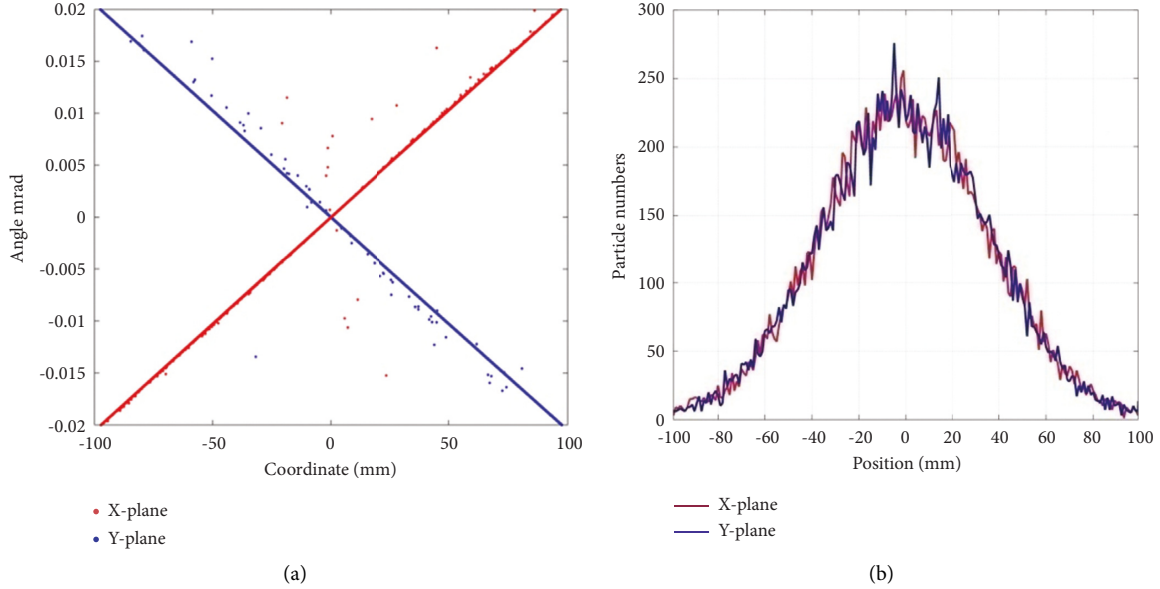


FIGURE 3: Proton beam at object plane. (a) Coordinate-angle correlations. (b) beam intensity distribution.

inverse problem in our previous work [19]. Figure 2 shows the flowchart of the genetic algorithm.

As shown in Figure 2, four parameters  $L$ ,  $G$ ,  $S$ , and  $D$  of Zumbro lens are represented by a randomly initialized binary vector chromosome. The domains of these variables are set as  $G \leq 10$  Tesla/m,  $L \in (0.5/\text{m}, 8/\text{m})$ ,  $S \in (3/\text{m}, 16/\text{m})$ , and  $D \in (1.5/\text{m}, 8/\text{m})$ . In each generation (evolution iteration procedure), a population with 70 individual chromosomes is used. Then, population evolution processed by three major operators (selection operator, crossover operator, and mutation operator). In the first iteration, the evolution step is skipped because fitness values are not calculated yet.

Fitness function  $OF1 + OF2$  is employed to evaluate the performance (fitness) of each chromosome. The first one,  $OF1$ , gives the motivation to minimize the  $m'_{12}$ . The second one,  $OF2$ , functions as constraints. The constant weights  $C1$  and  $C2$  are carefully set to guarantee the effectiveness of the constraints in the optimization.

The fitness value of each individual is then feedback to the evolution step. In this step, the Elitist [18] model used in a selection operator is to make sure the survival of the best individual. The crossover operator performs the inheritance and multiplication of chromosomes. The mutation operator offers the new chromosomes, which may improve the evolution. All in all, with a higher fitness value, the individual has more chance to keep its characteristic gene to next generation. Then, the population evolves from generation to generation until the best fitness is no more improved. A parameter set approximating the best is obtained consequently.

**2.2.4. Zumbro Lens for 20–50 GeV/c Protons.** The Zumbro systems suitable for 20 to 50 GeV/c protons are optimized. The results are listed in Table 1. The best parameter set practically contains the maximum intensity of magnetic field

( $G$ ) and the minimum value of  $D$  and  $S$ . It may be caused by the limitation of the quadrupole inner radius. As shown in Figure 1, in each quadrupole section, the trace of protons should be inside the quadrupole inner radius. The improvement on magnetic intensity  $G$  will decrease the offset by which proton trace is turned around. Therefore, the quadrupole with a limited radius desires a high magnetic intensity to avoid the bombarding of protons.

A tungsten slab with an areal density of  $200 \text{ g/cm}^2$  is taken as the object. The corresponding chromatic aberrations for difference cases are calculated and given in Table 1. The fourth column offers the calculated full-width at half maximum (FWHM) of the chromatic aberration induced blur. As a comparison, Geant4 is employed to simulate FWHM which can be found in the fifth column.

**2.3. Diffuser and Matching Lens.** As shown at far left of Figure 1, the upstream diffuser works together with the matching lens. The diffuser provides a desired position-angle correlation beam for matching lens. The basic structure of matching lens consists of three quadrupoles combining with four drifts. The matching lens has two functions. The first one is also to provide a proton beam with desired coordinate-angle correlation for Zumbro lens. The second is to expand the beam size to a fully illuminate object. There are 9 parameters for matching lens:  $D_{2,3,4}$ ,  $T_{1,2,3}$ , and  $G_{1,2,3}$ . The transfer of a proton in matching lens of X-plane has the form:

$$\begin{pmatrix} A \cdot X_0 \\ w \cdot A \cdot X_0 \end{pmatrix} = \begin{pmatrix} Mm_{11} & Mm_{12} \\ Mm_{21} & Mm_{22} \end{pmatrix}_{\text{Matching}} \begin{pmatrix} X_0 \\ w_0 \cdot X_0 + \phi_{\text{diffuser}} \end{pmatrix}, \quad (8)$$

TABLE 1: Optimized parameters.

Momentum/ GeV/c	L/m ( $S = 3$ m, $D = 1.5$ m, $G = 10$ Tesla/m)	$m_{12} \times \delta \times \theta$ (mm)	Calculated FWHM (mm)	G4 simulated FWHM (mm)
20	2.5978	1.363	3.2	2.6
25	3.1054	0.99	2.33	1.95
30	3.4	0.73	1.72	1.35
40	4.098	0.518	1.22	0.9
50	4.724	0.4	0.94	0.65

where  $A$  is the amplification factor of matching lens;  $w$  is the required correlation at the object plane;  $w_0$  is the correlation when the proton is at the entrance of the matching section; and  $\phi_{\text{diffuser}}$  is average scattering angle of proton in diffuser. The value of  $w_0$  not only involves in the matching lens optimization but also closely relates to the thickness of the diffuser.

Compared to the distance from matching lens to the diffuser, the beam size on diffuser is small which can be approximated as a point. Therefore,  $w_0$  equals to the reciprocal of the draft from a diffuser to matching lens ( $D_1$ , as shown in Figure 1).  $w_0$  is expected to have a positive correlation with the thickness of the diffuser:

$$w_0 \propto T_{\text{diffuser}}, \quad w_0 = \frac{1}{D_1}, \quad (9)$$

To decrease the chromatic aberration caused by the diffuser, a thinner diffuser should be used. However, it results in a large distance between the matching lens and diffuser. Therefore, apart from the correlation and amplification, a reasonable value of  $w_0$  should be carefully selected in the optimization about matching lens.

With a thin diffuser,  $\phi_{\text{diffuser}}$  is close to zero, and formula (8) can be expressed as follows:

$$\begin{cases} Mm_{11} + w_0 \cdot Mm_{12} = -A, \\ Mm_{21} + w_0 \cdot Mm_{22} = -w \cdot A. \end{cases} \quad (10)$$

The equation for  $y$  plane is similar, but the amplification factor is  $A$ . Formula (10) acts as the constraints in the optimization for the matching lens and diffuser.

The value of  $w$  is expected as 0.205 for the optimized Zumbro lens. The goal of the matching lens design is to obtain a higher amplification factor. To ensure a thin diffuser and an available drift length, the domain of  $w_0$  is set to be from 0.1 to 0.13. The overall length is limited within 30 meters. GA is employed to obtain a matching lens pursuing a 10 times amplification. All the optimized parameters are listed in Table 2.

Two issues should be noted for the data in Table 2. As mentioned for equation (9) that  $w_0 = 1/D_1$ , it is made based on point source assumption. Therefore,  $1/w_0$  is just an initial value of  $D_1$ . Geant4 is employed to obtain the exact value of  $D_1$  by repetition simulations. The secondary issue is relevant to the thickness of the diffuser. The designed amplification factor is 10 and the radius of FOV equals to 65 mm.

TABLE 2: Parameters of an optimized diffuser and matching lens.

Drifts (m)	$D_1 = 7.95$	$D_2 = 0.70$	$D_3 = 1.90$	$D_4 = 2.00$
Magnetic thickness (m)	$T_1 = 5.72$	$T_2 = 6.17$	$T_3 = 2.65$	~
Magnetic density (tesla/m)	$T_1 = 5.72$	$T_2 = 6.17$	$T_3 = 2.65$	~
W diffuser thickness (mm)	$T_{\text{diff}} = 1.5$	~	~	~

Therefore, the beam scale at the entrance plane of matching lens is expected to equal to or larger than 6.5 mm in radius. This beam scale is produced by the diffuser.

The object is often located at the center of FOV. To use the proton beam efficiently, the proton intensity at the center of illuminating beam should be higher than that at the edge of FOV. Here, proton intensity at the FOV edge is assumed to be 20% of the maximum value. Then, angular deviation  $\theta_0$  induced by a diffuser can be calculated by the following:

$$\theta_0 = \sqrt{\frac{\theta^2}{-2 \cdot \ln(0.2)} - \delta^2}, \quad (11)$$

where  $\delta$  is the angular deviation of the initial beam. Its value is assumed as 0.05 mrad. Then, the expected  $\theta_0$  is about 0.44 mrad. In a pure material, the angular deviation  $\theta_0$  induced by MCS can be calculated by using the following formula [22]:

$$\theta_0 = \frac{13.6 \text{ MeV}}{\beta c p} \sqrt{\frac{T_{\text{diff}}}{X} \left( 1 + 0.038 \frac{T_{\text{diff}}}{X} \right)}, \quad (12)$$

where  $p$  is the proton momentum,  $\beta c$  is the velocity,  $T_{\text{diff}}$  is diffuser thickness, and  $X$  is radiation length in material. With  $\theta_0 = 0.44$  mrad, thickness of the tungsten diffuser  $T_{\text{diff}}$  is calculated as 1.5 mm. Geant4 simulation shows that the fraction of momentum spreading caused by this diffuser is on order of 0.01%.

Designed diffuser, matching lens, and Zumbro lens were assembled as a whole system and modeled by Geant4. Then, the proton passing through the diffuser and magnetic lens is simulated. The obtained coordinate-angle correlations for both  $X$  and  $Y$  plane at the object plane are given in Figure 3(a). It coincides with the design. The simulation also shows that over 95% of protons can pass through this whole system. Figure 3(b) presents the beam distribution at the object plane. At the edge of FOV, the proton flux is about 20% to the maximum value which is also consistent with the design.



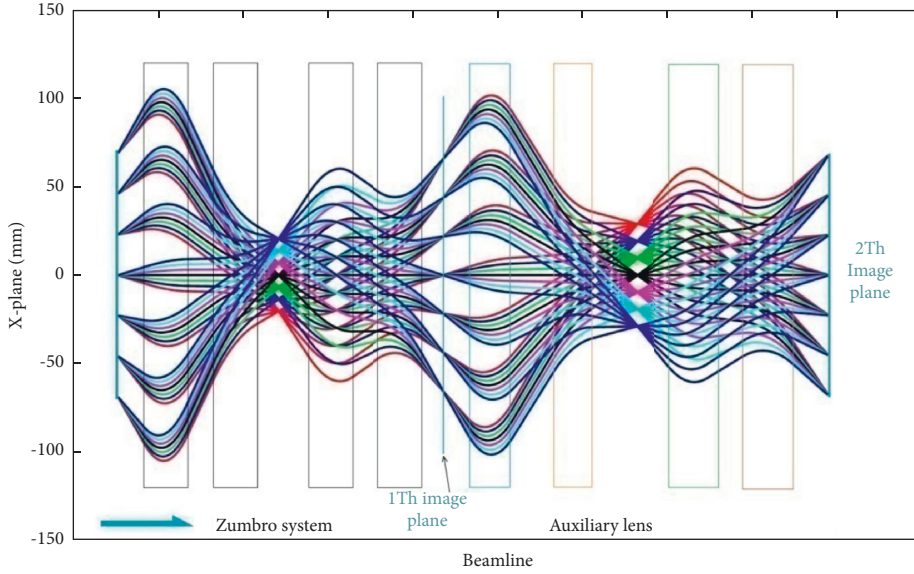


FIGURE 4: The structure of auxiliary lens and beam trajectory.

### 3. Auxiliary Lens for the Zumbro System

As shown in formula (1), the chromatic aberration is determined by the fractional momentum deviation ( $\sigma$ ) and the angular deviation ( $\phi$ ) from the ideal position-angle correlation line and the value of  $m'_{12}$ . The Zumbro lens is optimized according to a reference momentum. To reduce the value of  $\sigma$ , the reference momentum can be selected based on the momentum distribution when the proton leaves the object. For example, when a proton has penetrated a  $200 \text{ g/cm}^2$  tungsten slab, its momentum will distribute in a narrow range. Smaller chromatic aberration can be achieved if the reference momentum is adjusted to be at or nearby this range. However, for object with an irregular shape and areal density, adjusting the reference momentum cannot have the same effect on suppressing chromatic aberration as it is used for a slab shape object.

A new lens system named “auxiliary” is first proposed and shown in Figure 4. It has four different quadrupoles and located downstream of Zumbro lens (reference energy  $E_0$ ). The auxiliary lens is designed for the protons with  $E_1$  energy. Transfer matrix of these protons in Zumbro and auxiliary system has the following form:

$$M_{(E_1)} = MZ^n_{(E_0, E_1)} \cdot MA_{(E_1)} = \begin{vmatrix} 1 & 0 \\ 0 & 1 \end{vmatrix}, \quad (13)$$

where  $n$  means the number of Zumbro sections and MA and MZ are the transfer matrices of the incident proton in the auxiliary lens and the designed Zumbro lens, respectively. The auxiliary lens has 13 parameters including four magnetic field grads, four magnetic field lengths, and five drifts. The goal of GA optimization is to searching best parameter set. With these parameters, the transfer matrix of protons for both X and Y plane equals to identity matrix, as given in Formula (13).

Theoretically, by the Zumbro lens system as shown in Figure 4, inverting identity imaging without chromatic aberration can be achieved for  $E_0$  proton at 1Th image plane. At the 2Th image plane,  $E_1$  proton will be refocused without chromatic aberration by auxiliary lens.

Because proton energy varies from place to place on the image due to the areal densities of object and consequence proton energy loss, the  $E_0$  proton dominant area on 1Th image has the minimum chromatic aberration. On 2Th image plane produced by auxiliary lens, the area corresponding to  $E_1$  proton is not overlapped with that of  $E_0$  proton on 1Th image. It means that auxiliary lens can offer an extra area with minimum chromatic aberration.

Two objects are used to show the performance of auxiliary. The first sample is a tungsten slab with 28 vacancies. To avoid the thickness effect, the slab thickness is set to 1 cm. As shown in Figure 5, this slab consists of two parts, the top and the bottom half. Densities of these two parts are designed artificially as  $200 \text{ g/cm}^3$  (red) and  $170 \text{ g/cm}^3$  (blue), respectively. Both parts have the same geometry and vacancy pattern. In each part, two sets of 7 vacancies can be found on left and right. The vacancy widths are 0.5 mm and 1 mm, respectively. The thickness of the 7 vacancies varies from 1 mm to 10 mm by 1.5 mm intervals.

20 GeV/c proton beam is employed. The reference momentum for Zumbro lens is designed as 19.78 GeV/c according to the simulated energy loss of this proton in the slab. At the 1Th image plane (see Figure 4), the obtained image provided by the Zumbro lens is shown in Figure 6(a). The auxiliary lens is designed for 19.76 GeV/c protons. The corresponding image captured at 2Th image plane can be found in Figure 6(b).

As shown in Figure 6(a), if a proton passes through the thickest vacancy (10 mm like a hole), its scattered angle and consequent chromatic aberration blur are close to zero. At the top part, when the protons transmit 8.5 mm thick vacancy, as

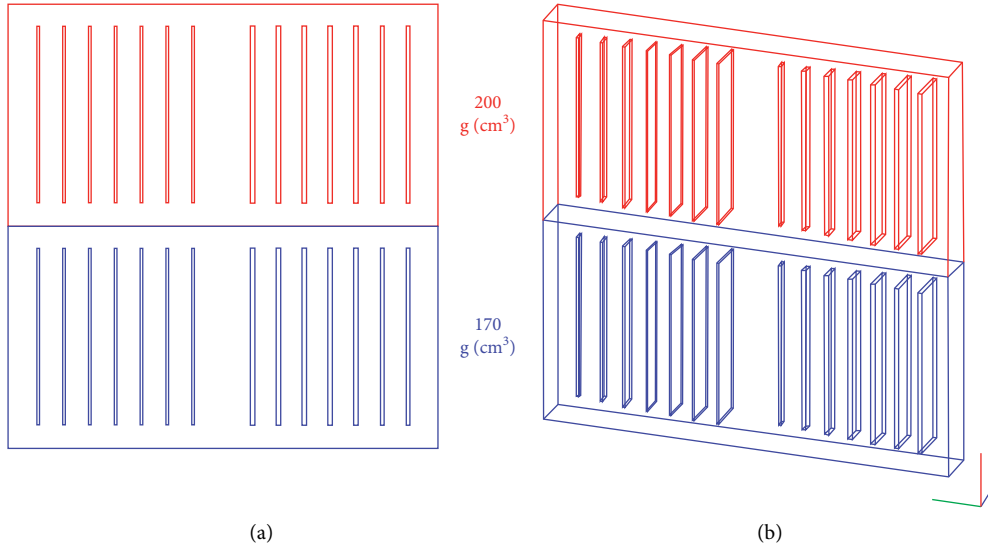


FIGURE 5: The geometry of slab object. (a) Beam eye view. (b) Oblique view.

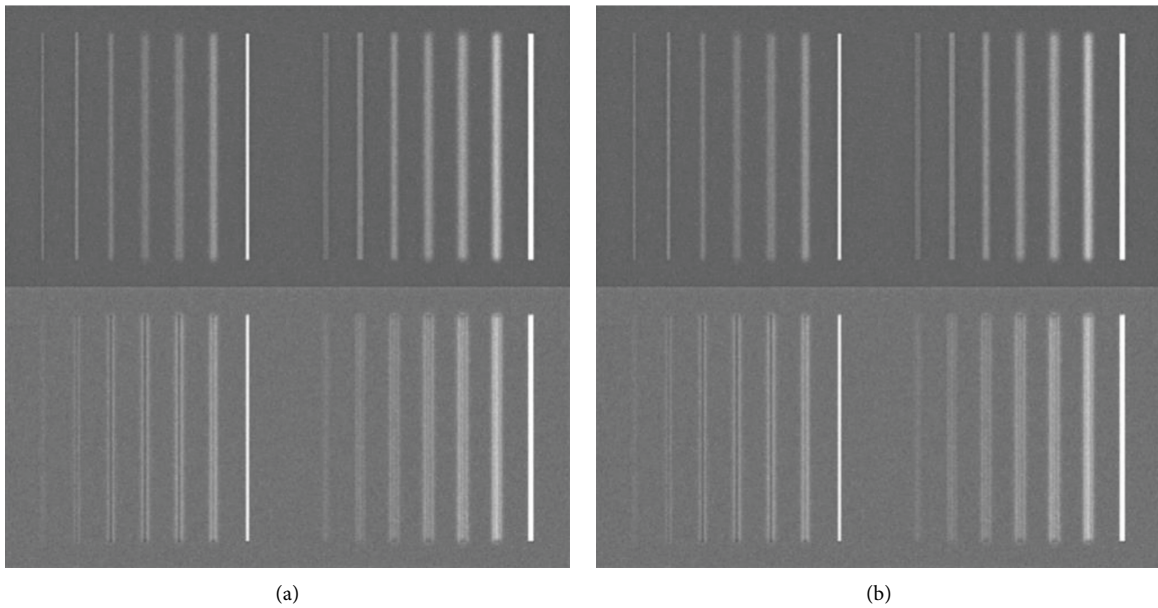


FIGURE 6: Recorded image of the slab object with the same proton beam. (a) Given by the Zumbro system (19.78 GeV). (b) Provided by auxiliary lens (19.76 GeV).

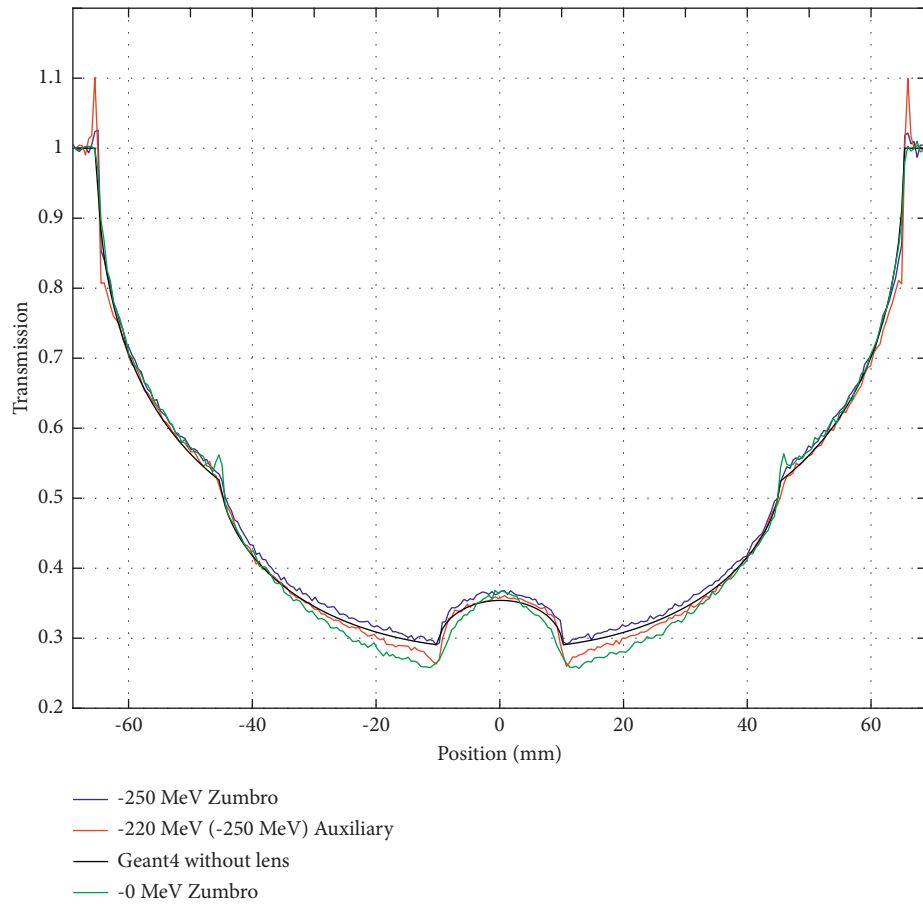
it penetrates the 1.5 mm slab material, the chromatic aberration blur is the largest. Apart from the thickest vacancy, minimum blur is found when vacancy is 2.5 mm (7.5 mm material with 150 g/cm<sup>2</sup> areal density) in thickness. It is because the momentum of the proton, which has penetrated 7.5 mm thick material, is close to the designed reference value of Zumbro lens. Compared to the top part, at the bottom, 1 mm thick vacancy (leftmost one) is more clearly. It is because the difference of areal density between top and bottom part.

In Figure 6(b), the thinnest vacancy at the leftmost of the top half is more clearly imaged compared to that in Figure 6(a). It is because auxiliary lens is designed for

19.76 GeV/c protons whose momentum is smaller than the reference value 19.78 GeV/c of Zumbro lens. Therefore, the proton which loses more energy in the object is expected to be better imaged by the auxiliary lens.

Both Zumbro and auxiliary lens have good imaging performance for their reference protons, respectively. Therefore, a new image can be generated using the information of the two images given by Zumbro lens and auxiliary lens. The obtained chromatic aberration will be evidently smaller than that obtained by only Zumbro lens.

Another object with complicated areal density distribution is employed. The shape of this object is an iron sphere



(a)



(b)

FIGURE 7: Cross-sectional distribution of sphere object.  $-250$  MeV means the reference momentum is  $250$  MeV lower than that of the incident proton ( $20$  GeV/c). (a) Cross-sectional distribution. (b) Residual error.



with bubble shape vacancy at the center. The momentum distribution of the emitted protons is more complicated than the slab object. According to the energy loss of 20 GeV/c proton in this object, the reference momentum of the Zumbro and auxiliary lens are designed as 19.75 GeV/c and 19.78 GeV/c, respectively. Geant4 code is employed for simulation and cross-sectional transmission distributions obtained by Zumbro and auxiliary lens are presented in Figure 7.

The actual attenuation length is determined by the removal cross section. Because the removal cross section varies with material components, object thickness, and the acceptance angle of the lens [8], it is hard to obtain by a simple calculation. Geant4 is therefore employed to calculate the ideal transmission at different positions which can be found in Figure 7(a) (labeled as Geant4 without lens).

As a comparison, another Zumbro lens with 20 GeV/c reference is simulated and given in Figure 7(a) as well. Figure 7(b) shows the residual of these distributions compared to the ideal one (Geant4 without lens).

The energy loss of the proton is different from place to place. The reference momentum of the lens should be varying with the position. For example, to the thickest part locating at 10–20 mm, the reference momentum should be set as 19.75 GeV/c (250 MeV lower than 20 GeV/c). At the center or other place shielded by less areal density, a higher momentum ranging from 19.77 GeV/c to 19.80 GeV/c acts better as the reference value.

As shown in Figure 7(b), the transmission residual of 19.75 Zumbro lens is the smallest at the position locating at 10–20 mm away from the center. At the rest positions with 0–10 mm and 20–60 mm distance away from the center, the transmission residual provided by the auxiliary lens is the smallest. If two images given by Zumbro and auxiliary lens are processed properly according to the momentum deviation and corresponding area, the residual error of the combined transmission is only few times 0.1%.

#### 4. Conclusion

All parts of proton radiography including the Zumbro lens, matching lens, and diffuser are studied. To suppress chromatic aberration-induced blurring, key parameters of the system are optimized under certain constraints. GA is employed as the optimizer. A new lens system called auxiliary lens is first proposed. Combined with an optimized Zumbro lens, an extra auxiliary lens can further decrease the remaining chromatic aberration. Monte Carlo simulation shows that this proposed lens can decrease chromatic aberration blurring and improve the radiography image evidently. The residual error of the obtained transmission is only few times 0.1% for a very thick object.

#### Data Availability

The data used to support the findings of this study are available from the corresponding author on request.

#### Conflicts of Interest

The authors declare that they have no conflicts of interest.

#### Acknowledgments

This work was supported by the National Natural Science Foundation of China (No. 11805018).

#### References

- [1] C. T. Mottershead and J. D. Zumbro, "Magnetic optics for proton radiography," in *Proceedings of the 1997 Particle Accelerator Conference*, pp. 1397–1402, Vancouver BC, Canada, May 1997.
- [2] A. Gavron, C. L. Morris, H. J. Ziock, and J. D. Zumbro, "Proton radiography," *Los Alamos National Report*, 1996.
- [3] J. F. Amann, C. J. Espinoza, and J. J. Gomez, *High-energy Test of Proton Radiography Concepts*, Los Alamos National Laboratory Document LA-UR, Washington, DC, USA, 1997.
- [4] A. J. Toepfer, "A review of accelerator concepts for the advanced hydrotest facility," in *Proceedings of the LANAC98*, Chicago, IL, USA, August 1998.
- [5] H. J. Ziock, K. J. Adams, K. R. Alrick et al., "The proton radiography concept," *Los Alamos National Laboratory*, 1998.
- [6] C. L. Morris, "Proton radiography for an advanced hydrotest facility," *Los Alamos National Report*, 2000.
- [7] B. Fishbine, "Proton radiography sharper —X-ray vision for hydrotests," *The Winter 2003 Issue of Los Alamos Research Quarterly*, Los Alamos National Laboratory, Mexico, MX, USA, 2003.
- [8] C. L. Morris, E. Ables, K. R. Alrick et al., "Flash radiography with 24 GeV/c protons," *Journal of Applied Physics*, vol. 109, no. 10, Article ID 104905, 2011.
- [9] T. Wei, G.-J. Yang, J.-D. Long, and J.-S. Shi, "Image blur in high energy proton radiography," *Chinese Physics C*, vol. 37, no. 6, Article ID 068201, 2013.
- [10] S. K. L. Sjuve, F. G. Mariam, F. E. Merrill, and C. L. A. Morris, "High order magnetic optics for high dynamic range proton radiography at a kinetic energy of 800 MeV," *Review of Scientific Instruments*, vol. 87, no. 1, Article ID 015110, 2016.
- [11] F. E. Merrill, "Flash proton radiography," *Reviews of Accelerator Science and Technology*, vol. 08, pp. 165–180, 2015.
- [12] M. S. Freeman, J. C. Allison, E. F. Aulwes et al., "Dark field proton radiography," *Applied Physics Letters*, vol. 117, no. 14, Article ID 144103, 2020.
- [13] Y. M. Antipov, A. G. Afonin, A. V. Vasilevskii et al., "A radiographic facility for the 70-GeV proton accelerator of the institute for high energy physics," *Instruments and Experimental Techniques*, vol. 53, no. 3, pp. 319–326, 2010.
- [14] A. V. Maksimov, N. E. Tyurin, and Y. S. Fedotov, "Optical system of the proton bombarding setup on the U-70 accelerator at the institute for high energy physics," *Technical Physics*, vol. 59, no. 9, pp. 1393–1399, 2014.
- [15] P. J. Bryant, *AGILE, a Tool for Interactive Lattice Design*, CERN, Geneva, Switzerland, 2000.
- [16] M. Berz, *COSY INFINITY Reference Manual*, Lawrence Berkeley National Laboratory, Berkeley, CA, USA, 2010.
- [17] J. D. Zumbro, A. Acuff, J. S. Bull, H. G. Hughes, R. E. Prael, and E. C. Selcow, "Proton radiography applications with MCNP5," *Radiation Protection Dosimetry*, vol. 117, no. 4, pp. 447–452, 2005.

- [18] M. Zbigniew, *Genetic Algorithms + Data Structures = Evolution Programs*, Springer, Berlin, Germany, 1999.
- [19] T. Zhang, H. Hu, Q. Jia et al., “Genetic algorithms applied to reconstructing coded imaging of neutrons and analysis of residual watermark,” *Review of Scientific Instruments*, vol. 83, no. 11, Article ID 113505, 2012.
- [20] J. Allison, K. Amako, J. Apostolakis et al., “Recent developments in Geant4,” *Nuclear Instruments & Methods in Physics Research, Section A*, vol. 835, 2016.
- [21] L. Jian-qin, *The Optics of Charged Particle Beams*, High Education Press, Beijing, China, 2004.
- [22] Y. Yan, L. Sheng, Z. Huang et al., “Simulation of proton radiography terminal at the institute of modern physics,” *Laser and Particle Beams*, vol. 33, no. 3, pp. 439–447, 2015.